

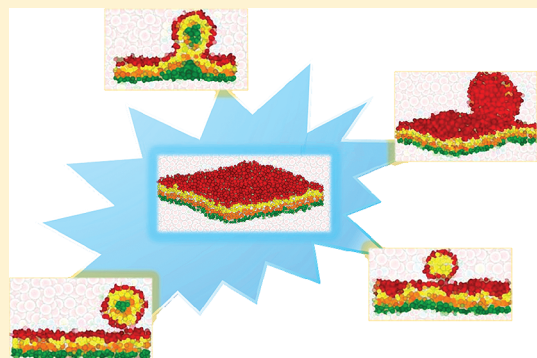
Curvature Changes of Bilayer Membranes Studied by Computer Simulations

Kai Yang,[†] Bing Yuan,[†] and Yu-Qiang Ma^{*,‡,†}

[†]Center for Soft Condensed Matter Physics and Interdisciplinary Research, Soochow University, Suzhou, 215006, China

[‡]National Laboratory of Solid State Microstructures and Department of Physics, Nanjing University, Nanjing, 210093, China

ABSTRACT: The deformation behaviors and corresponding curvature changes of bilayer membranes composed of amphiphiles are of biological importance and have potential industrial applications. Here, we study the curvature changes of bilayer membranes under the area-difference and spontaneous curvature effects with dissipative particle dynamics. By varying the relative quantity of the amphiphiles in two monolayers or the head–head interaction between the amphiphiles within each monolayer, rich morphological responses of the membranes are obtained. We find that some important factors such as the ability of amphiphiles to change their configurations in different membrane (crowded or sparse) environments and the coupling between the two monolayers, which are not included in the theoretical models, actually affect the deformation behavior of the membrane. Furthermore, the relationship between membrane deformation and fission (such as the transition from budding to scission of the bilayer) is also discussed, which is helpful in deeply understanding the fission event of the cell membrane.



INTRODUCTION

Amphiphiles (e.g., lipids, surfactants, or diblock copolymers) can self-assemble into ordered bilayers. These bilayer membranes are soft and have various morphologies under different circumstances, which provide the simple model for living cells and have huge potential applications in drug delivery and gene therapy, etc.^{1–4} Therefore, for both basic scientific research and industrial applications, it is of fundamental importance to explore the deformation mechanism of a bilayer membrane.

Undoubtedly, a cell membrane composed of lipids is the most important bilayer in biological systems.⁴ Especially, the deformation behaviors of a cell membrane are the prerequisites for some cellular activities such as cell movement, division, and the budding and fusion processes of membrane trafficking, etc.^{5,6} The asymmetry in the two monolayers of a bilayer in composition or lipid quantity, which is the intrinsic character of a cell membrane⁴ or produced by flip-flop events mediated by floppases,⁷ is regarded as a vital factor in determining the curvature characters of a cell membrane.⁴ On the basis of this perspective, many theoretical models (e.g., the area-difference elasticity model and the spontaneous curvature model) and computer simulations have been applied to examine the deformation behavior of the membrane.^{8–16}

Additionally, much attention has been paid to surfactant or diblock copolymer bilayer membranes due to the possibilities in chemical modification to the components and better material properties than lipid assemblies.^{17,18} For these amphiphile bilayer membranes, shape deformation behaviors similar to lipid bilayers are observed in both experimental and theoretical

investigations.^{2,18–20} However, we are still far from a full physical understanding of the deformation mechanism of a bilayer membrane, as some issues to date are still unclear. For example, besides the area-difference and spontaneous curvature effects, is there any other factor influencing the curvature change of a bilayer?²¹ Is line tension indispensable for the occurrence of fission in a planar membrane?^{16,22}

In this work, we systematically study the deformation behaviors and curvature changes of a planar bilayer membrane composed of amphiphiles under the influence of area-difference and spontaneous curvature effects by using dissipative particle dynamics (DPD). Various morphological responses of the bilayers are observed in the simulations. Additionally, a shape-fitting method is applied to quantitatively analyze the curvature changes of the bilayers, which may further improve our understanding of the deformation mechanism of the membrane beyond the theoretical models. Especially, our simulations predominantly prove that fission is able to occur in a planar bilayer without the help of line tension and will be helpful to deepen the understanding of the molecular mechanism of fission in the cell.

SIMULATION METHOD AND MODEL

DPD is a coarse-grained computer simulation technique with hydrodynamic interaction,²³ which has been used to study the deformation behaviors of bilayer membranes and related

Received: March 26, 2012

Revised: May 28, 2012

Published: May 30, 2012

phenomena.^{24–29} In the DPD technique, each DPD bead is composed of a group of atoms or molecules. The evolution of the position and velocity of the DPD bead i , (\vec{r}, \vec{v}_i) , obeys Newton's equation of motion

$$\frac{d\vec{r}_i}{dt} = \vec{v}_i, \quad \frac{d\vec{v}_i}{dt} = \frac{\vec{f}_i}{m}$$

One main feature of the DPD is that the interaction between two beads is soft, which can be denoted as $\vec{F}_{ij}^C = a_{ij}(1 - (r_{ij}/r_c))\vec{e}_{ij}$. Here, a_{ij} represents the maximum repulsion interaction between beads i and j , $\vec{r}_{ij} = \vec{r}_i - \vec{r}_j$, $r_{ij} = |\vec{r}_{ij}|$, and $\vec{e}_{ij} = \vec{r}_{ij}/r_{ij}$. Furthermore, random force \vec{F}_{ij}^R and friction \vec{F}_{ij}^D are applied to each pair of neighboring beads to keep the momentum locally conserved and produce the hydrodynamic effect. They can be taken as $\vec{F}_{ij}^D = -\gamma(1 - (r_{ij}/r_c))^2(\vec{e}_{ij} - \vec{v}_{ij})\vec{e}_{ij}$, and $\vec{F}_{ij}^R = (2\gamma k_B T)^{1/2}(1 - (r_{ij}/r_c))\xi_{ij}\Delta t^{1/2}\vec{e}_{ij}$, respectively (here, $\vec{v}_{ij} = \vec{v}_i - \vec{v}_j$ is the relative velocity between beads i and j ; γ is the strength of friction; and ξ_{ij} is a symmetric random variable with zero mean and unit variance). The cutoff radii of all forces are r_c . Our simulations adopt a modified velocity-Verlet integration algorithm²³ and the simulation time step $\Delta t = 0.02\tau$ ($\tau = [mr_c^2/k_B T]^{1/2}$). In addition, the cutoff radius r_c , bead mass m , and temperature $k_B T$ are chosen as the simulation units.

An amphiphile is modeled as a linear chain with two hydrophilic head beads (h) and five hydrophobic tail beads (t) in the simulations. A harmonic spring is applied to connect the neighboring beads in a single molecule. The spring constant is $k_s = 128k_B T/r_c$, and the equilibrium bond length is set to $l_0 = 0.5r_c$. To ensure the rigidity of hydrocarbon chains, a three-body bond angle potential U_b with force constant $k_b = 5k_B T/r_c$ and the preferred angle $\varphi_0 = 180^\circ$ is applied: $U_b = k_b(1 - \cos(\varphi - \varphi_0))$. Additionally, water is explicitly included in the system as the solvent (w). The interaction parameters a_{ij} between beads are chosen according to their characters (i.e., hydrophobicity or hydrophilicity, Table 1).

Table 1. Values of a_{ij} ($k_B T/r_c$)^a

a_{ij}	w	h_{upper}	t_{upper}	h_{bottom}	t_{bottom}
w	25	25	95	25	95
h_{upper}	25	a_{hh_upper}	95	25	95
t_{upper}	95	95	25	95	25
h_{bottom}	25	25	95	a_{hh_bottom}	95
t_{bottom}	95	95	25	95	25

^aThe “upper (bottom)” in the subscript represents the amphiphile in the upper (bottom) monolayer of the bilayer.

All simulations are performed in NVT ensembles with the periodic boundary conditions (unless special statements) at the temperature $k_B T = 1$. The size of the simulation box is $40r_c \times 40r_c \times 48r_c$. At the beginning of the simulation, an equilibrated planar bilayer with near zero surface tension is placed in the center of the simulation box (x - y plane), and the quantity of amphiphiles in each monolayer is 1975. However, to investigate the influence from the membrane asymmetry, the difference in amphiphile quantity between upper/bottom monolayers, as well as the interaction between the head beads of amphiphiles in each monolayer (see Table 1), can be changed. All simulations are carried out in 3×10^5 simulation steps and at least 3 independent runs.

To quantitatively analyze the curvature changes of the bilayer, a shape-fitting method is performed.^{28,30} In short, the

bilayer is divided into $1r_c \times 1r_c$ vertical square prisms being parallel to the z axis. Thus, the positions of the mass centers of beads in every prism give an approximate shape of the whole bilayer. The mathematical expression for the best-fit surface is obtained through least-squares fitting as

$$z(x, y) = \sum_{i+j \leq 5} D_{i,j} x^i y^j \quad (1)$$

Thus, the curvature of each point, (x, y) , can be evaluated as

$$k_x = \left[\frac{(1 + (dz/dx)^2)^{3/2}}{d^2 z / dx^2} \right]^{-1},$$

$$k_y = \left[\frac{(1 + (dz/dy)^2)^{3/2}}{d^2 z / dy^2} \right]^{-1} \quad (2)$$

SIMULATION RESULTS

A. Influence of the Area-Difference Effect. Here, we will concentrate on the effect of the area difference between the two monolayers on the deformation of a bilayer membrane. The interaction parameter between the amphiphile heads within each monolayer is kept as $a_{hh_upper} = a_{hh_bottom} = 25k_B T/r_c$. On the basis of the ADE model, the energy of the area-difference effect can be taken as

$$E_b = \frac{\kappa}{2} \frac{\pi}{AD^2} (\Delta A - \Delta A_0)^2 \quad (3)$$

where κ is the elasticity constant; D is the bilayer thickness; A is the membrane surface area; and ΔA and ΔA_0 are the actual and preferred area difference between the two monolayers, respectively. E_b is the driving energy leading to the shape deformation of the bilayer. Thus, in the simulations, the area-difference effect can be produced by varying the relative quantity of amphiphiles in the two monolayers,^{25,31,32} defined as the upper-bottom number ratio $\gamma = (N_{\text{amphiphile_upper}})/(N_{\text{amphiphile_bottom}})$ here.

A variety of morphologies, including planar, curved, and budding bilayers, as well as the sheet caused by monolayer collapse, are observed in our simulations with different ratio γ (Figure 1a). For most cases of $\gamma > 1$ (i.e., the quantity of amphiphiles in the upper monolayer is larger than that in the bottom one, while $N_{\text{amphiphile_bottom}}$ is fixed to 1975), our observations are basically consistent with the ADE model: the curvature of the bilayer increases rapidly with increasing γ (Figure 1b), and correspondingly, the bilayer deforms to a curved one (as shown in Figure 1d). Even when γ reaches 1.3/1.0, a bud grows from the region where the membrane deforms most seriously; thereafter, a neck is formed (Figure 1e). However, the neck is so stable that no fission is observed even after a long time (more than 300 000 steps) in the simulations.

However, for some cases of γ (e.g., $\gamma \geq 1.4/1.0$ or $\gamma < 1$), abnormal morphological changes of the bilayer membranes are observed in the simulations. For example, when $\gamma \geq 1.4/1.0$, a monolayer sheet (i.e., a micelle bud) appears (Figure 1f). In this case, the upper monolayer deforms so rapidly and dramatically that the bottom monolayer cannot follow. As a result, the upper monolayer collapses to a sheet, while the bottom one keeps unchanged (Figure 1f). Such a sheet is stable in the simulations as well as the bud formation mentioned above. The comparison between the formation processes of a bud and a sheet (Figures 1e and f) indicates that the response of one monolayer to the structural or state change of the other

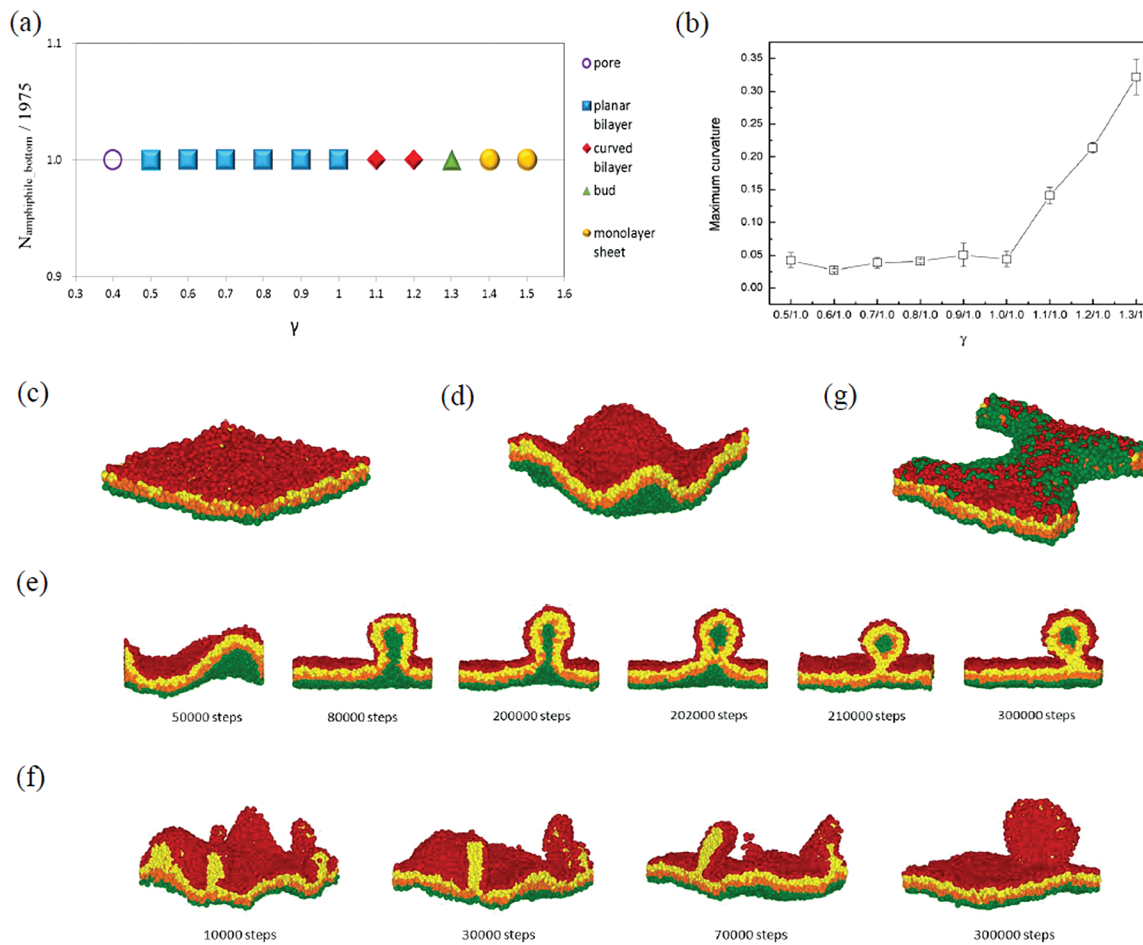


Figure 1. (a) Final morphologies of bilayers with different ratio γ . (b) The maximum values of the curvatures of bilayers with different γ (each value is averaged by three independent simulation runs). (c) Snapshot of a bilayer with $\gamma = 0.5/1.0$ ($t = 3 \times 10^5$ simulation steps). (d) Snapshots of a curved bilayer with $\gamma = 1.2/1.0$ ($t = 3 \times 10^5$ simulation steps). (e) The formation process of a bud when $\gamma = 1.3/1.0$ (cross section). (f) The collapsing process of the upper monolayer and the formation of a sheet when $\gamma = 1.4/1.0$. (g) Snapshot of a pore in a bilayer with $\gamma = 0.4/1.0$ ($t = 3 \times 10^5$ simulation steps). Red and yellow: the head and tail beads of amphiphile in the upper monolayer. Green and orange: the head and tail beads of amphiphile in the bottom monolayer.

one, namely, the coupling between the two monolayers, is crucial in determining the final morphology of a bilayer.

Interestingly, for the case of $\gamma < 1$ (i.e., the quantity of amphiphiles in the upper monolayer is less than that of the bottom one while $N_{\text{amphiphile bottom}}$ is fixed to 1975), the bilayer membrane keeps planar (Figure 1b), similar to the example shown in Figure 1c. It is noted that the flip-flop event rarely occurs in our simulations due to the relatively strong hydrophobic interaction among the tails of amphiphiles, so the area-difference effect should also be appropriate for the case $\gamma < 1$ according to the ADE model. However, our simulations show that the curvature changes of the bilayers under the two conditions (i.e., $\gamma > 1$ or $\gamma < 1$) are different. By comparing the structure of the bilayer of $\gamma < 1$ with the equilibrium one (Figure 2a), we infer that the difference in the ability of amphiphiles to change their configurations in various membrane environments (crowded or sparse) might be a dominating influential factor: for $\gamma < 1$, the amphiphiles in the upper monolayer can tilt themselves easily to occupy the extra monolayer space due to the loss of the molecules, although the tilt of them makes the upper monolayer thinner. Moreover, some amphiphiles in the bottom monolayer protrude their tails into the upper one (Figure 2a). These changes are also reflected by the composition distribution of the amphiphiles as

well (Figure 2b): the distance between the amphiphile heads in two monolayers reduces with the decrease of γ , and the distribution of the amphiphiles in the bottom monolayer moves obviously toward the upper one. Importantly, membrane tension induced by the asymmetry in amphiphile quantity appears (Figure 2c), which is the reflection of the configuration changes of amphiphiles in the bilayer ($\gamma < 1$) or the driving force for the deformation of the membrane ($\gamma > 1$). For $\gamma < 1$, the configuration changes of amphiphiles effectively compensate the area difference between the two monolayers, except the case of a small enough γ in which a pore is formed in the membrane (Figure 1g). However, for the bilayer with $\gamma > 1$, amphiphiles are impossible to change their configurations due to the crowded environment, thus the membrane has little room to accommodate the increased molecules and release the stress produced by the insertion, unless by deforming the bilayer. Therefore, we conclude that the different abilities of amphiphiles to change their configurations in various membrane environments strongly affect the area-difference effect of the bilayer and the membrane deformation behavior.

Furthermore, it is indicated by our simulations that the morphological changes of bilayer membranes are roughly independent of the changing manner of amphiphile quantity, in which amphiphiles can be inserted in or deleted from the

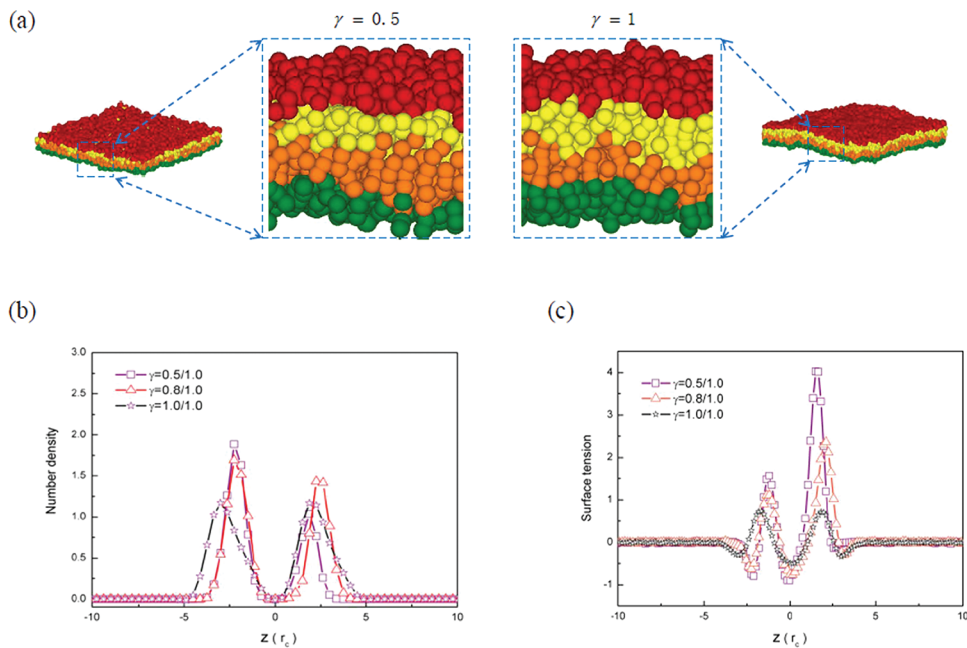


Figure 2. (a) Detailed snapshots of a bilayer with $\gamma = 0.5/1.0$ (left) and $\gamma = 1.0$ (right). (b) and (c) Number densities of the head beads and membrane tension profiles of the bilayers with various γ .

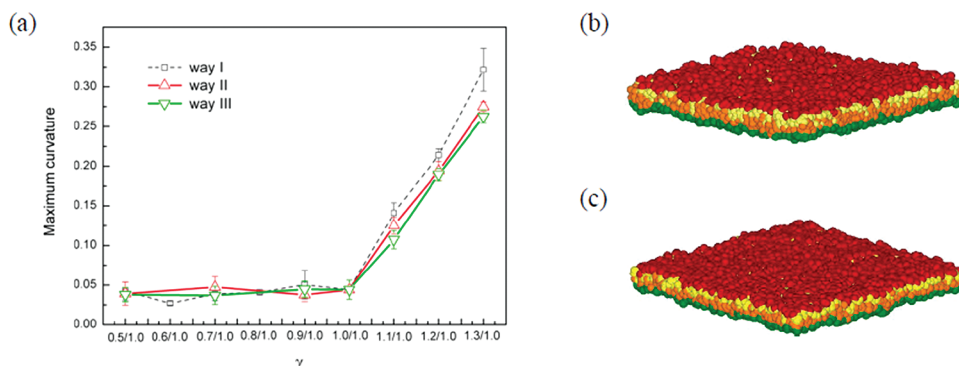


Figure 3. (a) Maximum values of the curvatures of bilayer membranes with different γ and various ways for the quantity changing of amphiphiles (Way I: amphiphile quantity of the upper monolayer varies directly at the beginning of the simulations as shown in Figure 1b; Way II: 18 amphiphiles insert or delete in every 500 simulation steps; Way III: 18 amphiphiles insert or delete in every 1000 simulation steps. Each value is averaged by three independent simulation runs). (b) and (c) Snapshots of bilayers with $\gamma = 0.5/1.0$ simulated under the quasi-periodic boundary condition and in *NPT* ensembles, respectively. All snapshots are obtained at $t = 3 \times 10^5$ simulation steps.

bilayer directly or step by step (Figure 3a). Additionally, to exclude the possible influence of simulation techniques, such as the boundary condition and simulation ensembles, additional DPD simulations are performed in a larger membrane system ($54r_c \times 54r_c \times 48r_c$) with two other simulation conditions: One is a “quasi-periodic boundary condition”, in which the amphiphiles in the boundary region of the membrane (whose thickness is $2r_c$ in our simulations) can be inserted or deleted to maintain the lateral membrane tension and mimic an open membrane;^{26,28} The other is *NPT* ensembles with a Berendsen barostat in which the size of the simulation box in the two dimensions of the membrane spanned can be altered to control the lateral pressure similarly as done by Deserno et al.²² Under these simulation conditions, similar curvature and morphological changes of bilayer membranes with γ as Figure 1 are observed. Especially, when $\gamma < 1$, the bilayer really keeps flat, as shown in Figures 3b and c. These results further indicate the significance of the changes of amphiphile configurations in the deformation behavior of a bilayer.

B. Influence of the Spontaneous Curvature Effect. The spontaneous curvature effect of a bilayer is also one of the important factors influencing the shape deformation of a membrane, whose contribution can be described as

$$E_b = \int dA \left[\frac{\kappa_c}{2} (C_1 + C_2 - C_0)^2 + \frac{\kappa'_c}{2} C_1 C_2 \right] \quad (4)$$

where κ_c and κ'_c are constants; C_1 and C_2 are two principal curvatures; and C_0 is the spontaneous curvature of the bilayer. In the simulations, the value of a_{hh} (i.e., the interaction between amphiphile heads) determines the mean distance between the amphiphile head-groups. Therefore, as introduced in the previous simulations,^{12,33} with the increase or decrease of a_{hh} , the “effective shape” (or packing state in the bilayer) of an amphiphile molecule, as well as the spontaneous curvature of a membrane, will be changed. By doing this, we observe different kinds of bilayer morphologies (see Figure 4a). Note that amphiphiles prefer to stay as a planar bilayer in our simulations

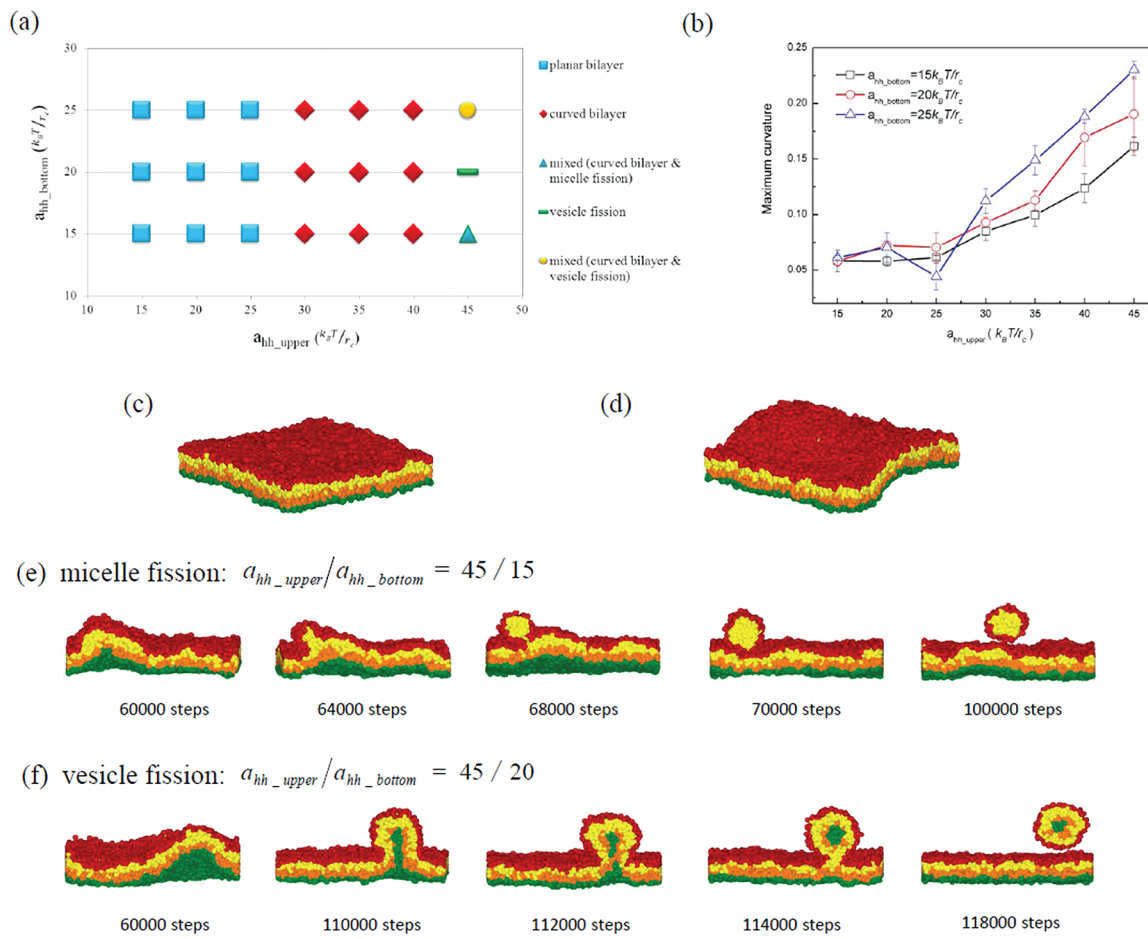


Figure 4. (a) Final morphologies of the bilayers under different a_{hh} . (b) The maximum curvatures of the bilayers with different a_{hh} (each value is averaged by four independent simulation runs). (c) and (d) Snapshots of bilayers with $a_{hh_upper}/a_{hh_bottom} = 15/25$ and $a_{hh_upper}/a_{hh_bottom} = 35/25$, respectively ($t = 3 \times 10^5$ simulation steps). (e) and (f) Formation processes of two types of fission (cross-section).

as $a_{hh} = 25k_B T/r_c$. Interestingly, fission can be observed in the simulations.

When a_{hh_upper} is larger than $25k_B T/r_c$, the deformation of the bilayer becomes obviously stronger (Figure 4b). This changing tendency is essentially in agreement with the spontaneous-curvature model: with the increase of a_{hh_upper} , the amphiphiles in the upper monolayer turn to be cone-shaped, leading to the increase of the spontaneous curvature effect and the deformation of the membrane.

However, when a_{hh_upper} is less than $25k_B T/r_c$, the membrane keeps planar (Figure 2b). Even with a similar Δa_{hh} ($\Delta a_{hh} = |a_{hh_upper} - a_{hh_bottom}|$), the morphological responses and the curvature changes of the bilayers are absolutely different (Figures 2c and d). In general, regardless of whether a_{hh_upper} is larger or less than $25k_B T/r_c$ in our simulations, the packing state of amphiphiles and the spontaneous curvature of the bilayer should be changed. However, when a_{hh_upper} decreases, amphiphiles turn to be inverted cone-shaped, and the upper monolayer becomes sparse, especially in the head region. Thus, we infer that the changes of amphiphile configurations under this condition would eliminate the spontaneous curvature effect of the bilayer, similarly to that in the case of $\gamma < 1$. This deduction is also helpful to understand some observations in our simulations. For example, with a similar a_{hh_upper} (e.g., $a_{hh_upper} = 30k_B T/r_c$ in Figure 4b), the deformation of the bilayer with a smaller a_{hh_bottom} (e.g., $a_{hh_bottom} = 15k_B T/r_c$) is weaker than that with a larger a_{hh_bottom} (e.g., $a_{hh_bottom} =$

$20k_B T/r_c$), although the former case has a larger Δa_{hh} . With a smaller a_{hh_bottom} , the stronger changes in amphiphile configurations compensate the spontaneous curvature effect, subsequently suppressing the deformation tendency of the membrane. Therefore, these results further demonstrate that the ability of amphiphiles to change the configurations in various membrane environments is important in determining the ultimate morphology of a membrane.

Furthermore, when a_{hh_upper} is large enough, two types of fission behaviors are observed. According to the formation of the daughter from the parent membrane in the fission process, i.e., a micelle or a vesicle, we name the phenomenon as a micelle-fission or a vesicle-fission (Figures 4e and f). Especially, the micelle-fission proceeds without the participation of the bottom amphiphiles. Due to the dependence of these fission behaviors on the varying of a_{hh_bottom} (Figure 4a), it is inferred that the coupling in deformation speed between the two monolayers might be important: When a_{hh_bottom} reduces to $15k_B T/r_c$, the deformation of the bottom monolayer is restrained by the configuration changes of amphiphiles in a sparse monolayer environment as mentioned above, while on the other hand, the upper monolayer tends to expand outward due to the rather larger a_{hh_upper} ($45k_B T/r_c$). As a result of this competition, a daughter micelle is generated from the upper monolayer without the participation of the bottom molecules. However, when a_{hh_bottom} increases to $20k_B T/r_c$, the bottom monolayer is able to follow the deformation of the upper one,

and consequently a daughter vesicle that contains a part of the bottom amphiphiles forms. Thus, the coupling between the two monolayers also affects the deformation behavior of the bilayer.

The transition from budding to scission of a bilayer membrane is an important step for the fission. Our simulations also give an insight into this transition, especially the stability of the neck. It is known that the neck of a bud can be stable in a lipid bilayer which has been confirmed by the results of theoretical models,^{34,35} experiments,^{16,36,37} and computer simulations.^{26,28,32} Usually, it is thought that the disruption of the neck requires the help of line tension along a domain.^{25,26,38,39} However, our results show that fission can occur easily (the formation and disruption of the neck can be realized within 1×10^4 simulation steps in our simulations) only if the effect of the molecular shape of the amphiphile is concerned. This is also reflected by experimental results of Imai et al.,¹⁶ which indicate that lipid shape indeed influences the morphological change of vesicle fission. Therefore, it can be concluded that the neck could be disrupted by changing the shape of the amphiphile, not just the line tension. Another interesting finding in our simulation is about the relationship between the deformation degree of the membrane and the transition. A strong deformation of the membrane would usually be thought to facilitate the transition from budding to scission of the membrane. However, by comparing the curvature changes of the membrane driven by the area-difference and the spontaneous curvature effects (Figures 1b and 3b), it is found that the former factor can deform the membrane much more dramatically, while only under the latter condition fission occurs. These results confirm that whether fission would occur or not mostly depends on the curvature changes in the local region (e.g., around the neck) but not the deformation degree of the whole membrane.

CONCLUSION

In summary, the curvature changes and deformation behaviors of bilayer membranes are investigated by computer simulations. Rich morphologies of the bilayers are obtained and analyzed. We find that the difference in the ability of amphiphiles to change their configuration in various membrane environments (e.g., crowded or sparse) has a strong influence on the deformation of the bilayer. Also, the coupling between the two monolayers is essential for the ultimate curvature characters of the membrane. However, both factors are overlooked by previous theoretical models.^{8–10,40} Our results provide a good supplement to the theoretical models and give a deeper insight into the deformation and fission mechanism of the cell membrane.

AUTHOR INFORMATION

Corresponding Author

*E-mail: myqiang@nju.edu.cn.

Notes

The authors declare no competing financial interest.

ACKNOWLEDGMENTS

This work was supported by the National Natural Science Foundation of China (Nos. 91027040, 11104192, 10974080, and 21106114) and the National Basic Research Program of China (No. 2012CB821500). K.Y. thanks the support of the Key Project of Chinese Ministry of Education (No. 210208), the Applied Basic Research Program (No. 2010CD091), and

the Science Foundation of Department of Education of Yunnan Province of China (No. 2010Z077). B.Y. thanks the China Postdoctoral Science Foundation (No. 201104557).

REFERENCES

- (1) Discher, D. E.; Eisenberg, A. *Science* **2002**, *297*, 967–973.
- (2) Christian, D. A.; Tian, A.; Ellenbroek, W. G.; Levental, I.; Rajagopal, K.; Janmey, P. A.; Liu, A. J.; Baumgart, T.; Discher, D. E. *Nat. Mater.* **2009**, *8*, 843–849.
- (3) Guida, V. *Adv. Colloid Interface Sci.* **2010**, *161*, 77–88.
- (4) Alberts, B.; Johnson, A.; Lewis, J.; Raff, M.; Roberts, K.; Walter, P. *Molecular Biology of the Cell*; Garland science, Taylor & Francis Group: New York, 2008.
- (5) McMahon, H. T.; Gallop, J. L. *Nature* **2005**, *438*, 590–596.
- (6) Doherty, G. J.; McMahon, H. T. *Annu. Rev. Biochem.* **2009**, *78*, 857–902.
- (7) Pomorski, T.; Menon, A. K. *Cell. Mol. Life Sci.* **2006**, *63*, 2908–2921.
- (8) Seifert, U. *Adv. Phys.* **1997**, *46*, 13–137.
- (9) Miao, L.; Seifert, U.; Wortis, M.; Dobereiner, H. G. *Phys. Rev. E* **1994**, *49*, 5389–5407.
- (10) Deuling, H. J.; Helfrich, W. *J. Phys. (Paris)* **1976**, *37*, 1335–1345.
- (11) Markvoort, A. J.; Smeijers, A. F.; Pieterse, K.; van Santen, R. A.; Hilbers, P. A. J. *J. Phys. Chem. B* **2007**, *111*, 5719–5725.
- (12) Markvoort, A. J.; Spijker, P.; Smeijers, A. F.; Pieterse, K.; van Santen, R. A.; Hilbers, P. A. J. *J. Phys. Chem. B* **2009**, *113*, 8731–8737.
- (13) (a) Yuan, B.; Xing, L. L.; Zhang, Y. D.; Lu, Y.; Mai, Z. H.; Li, M. *J. Am. Chem. Soc.* **2007**, *129*, 11332–11333. (b) Tian, W. D.; Ma, Y. Q. *Soft Matter* **2012**, *8*, 6378–6384.
- (14) Inaoka, Y.; Yamazaki, M. *Langmuir* **2007**, *23*, 720–728.
- (15) Bacia, K.; Schwille, P.; Kurzchalia, T. *Proc. Natl. Acad. Sci. U.S.A.* **2005**, *102*, 3272–3277.
- (16) Sakuma, Y.; Imai, M. *Phys. Rev. Lett.* **2011**, *107*, 198101.
- (17) Needham, D.; Nunn, R. S. *Biophys. J.* **1990**, *58*, 997–1009.
- (18) Discher, B. M.; Won, Y. Y.; Ege, D. S.; Lee, J. C. M.; Bates, F. S.; Discher, D. E.; Hammer, D. A. *Science* **2002**, *284*, 1143–1146.
- (19) Larsen, A. L.; Terentjev, E. M. *Macromolecules* **2006**, *39*, 9508–9518.
- (20) Yuan, Z.; Dong, S.; Liu, W.; Hao, J. *Langmuir* **2009**, *25*, 8974–8981.
- (21) Yang, K.; Ma, Y. Q. *Soft Matter* **2012**, *8*, 606–618.
- (22) Reynwar, B. J.; Illya, G.; Harmandaris, V. A.; Muller, M. M.; Kremer, K.; Deserno, M. *Nature* **2007**, *447*, 461–464.
- (23) Groot, R. D.; Rabone, K. L. *Biophys. J.* **2001**, *81*, 725–736.
- (24) Grafmüller, A.; Shillcock, J.; Lipowsky, R. *Phys. Rev. Lett.* **2007**, *98*, 218101.
- (25) Yamamoto, S.; Hyodo, S.-a. *J. Chem. Phys.* **2003**, *118*, 7937–7943.
- (26) Hong, B. B.; Qiu, F.; Zhang, H. D.; Yang, Y. L. *J. Phys. Chem. B* **2007**, *111*, 5837–5849.
- (27) (a) Yang, K.; Ma, Y. Q. *Nat. Nanotechnol.* **2010**, *5*, 579–583. (b) Ding, H. M.; Tian, W. D.; Ma, Y. Q. *ACS Nano* **2012**, *6*, 1230–1238.
- (28) Yue, T.; Li, S.; Zhang, X.; Wang, W. *Soft Matter* **2010**, *6*, 6109–6118.
- (29) Li, D. W.; Liu, X. Y.; Feng, Y. P. *J. Phys. Chem. B* **2004**, *108*, 11206–11213.
- (30) Hsin, J.; Gumbart, J.; Trabuco, L. G.; Villa, E.; Qian, P.; Hunter, C. N.; Schulten, K. *Biophys. J.* **2009**, *97*, 321–329.
- (31) Yang, K.; Shao, X.; Ma, Y. Q. *Phys. Rev. E* **2009**, *79*, 051924.
- (32) Ramachandran, S.; Kumar, P. B.; Laradji, M. *J. Chem. Phys.* **2008**, *129*, 125104.
- (33) Markvoort, A. J.; van Santen, R. A.; Hilbers, P. A. J. *J. Phys. Chem. B* **2006**, *110*, 22780–22785.
- (34) Lipowsky, R. *J. Phys. II (France)* **1992**, *2*, 1825–1840.
- (35) Chen, C.-M.; Higgs, P. G.; Mackintosh, F. C. *Phys. Rev. Lett.* **1997**, *79*, 1579–1582.

- (36) Dobereiner, H.-G.; Kas, J.; Noppi, D.; Sprenger, I.; Sackmann, E. *Biophys. J.* **1993**, *65*, 1396–1403.
- (37) Andes-Koback, M.; Keating, C. D. *J. Am. Chem. Soc.* **2011**, *133*, 9545–9555.
- (38) Cooke, I. R.; Kremer, K.; Deserno, M. *Phys. Rev. E* **2005**, *72*, 011506.
- (39) Ramachandran, S.; Laradji, M.; Kumar, P. B. *J. Phys. Soc. Jpn.* **2009**, *78*, 041006.
- (40) Lipowsky, R. *Nature* **1991**, *349*, 475–481.